The coding of valence and identity in the mammalian taste system

Li Wang[1,2], **Sarah Gillis-Smith**[1,2], **Yueqing Peng**[1,2], **Juen Zhang**[1,2], **Xiaoke Chen**[1,2,3], **C. Daniel Salzman**[2,4], **Nicholas J. P. Ryba**[5], and **Charles S. Zuker**[1,2]

[1]Howard Hughes Medical Institute and Departments of Biochemistry and Molecular Biophysics

[2]Neuroscience, Columbia College of Physicians and Surgeons, Columbia University, New York, NY 10032, USA

[4]Department of Psychiatry and New York State Psychiatric Institute, Columbia University, New York, NY 10032, USA

[5]National Institute of Dental and Craniofacial Research, National Institutes of Health, Bethesda, MD 20892, USA

Abstract

The ability of the taste system to identify a tastant (what does it taste like?) enables animals to recognize and discriminate between the different basic taste qualities[1,2]. The valence of a tastant (is it appetitive or aversive?) specifies its hedonic value, and the execution of selective behaviors. Here we examine how sweet and bitter are afforded valence versus identity. We show that sweet and bitter cortex project to topographically distinct areas of the amygdala, with strong segregation of neural projections conveying appetitive versus aversive taste signals. By manipulating selective taste inputs to the amygdala, we show that it is possible to impose positive or negative valence to a neutral water stimulus, and even to reverse the hedonic value of a sweet or bitter tastant. Remarkably, animals with silenced amygdala no longer exhibit behavior that reflects the valence associated with direct stimulation of taste cortex, or with delivery of sweet and bitter chemicals. Nonetheless, these animals can still identify and discriminate between tastants, just as wildtype controls do. These results help explain how the taste system generates stereotypic and predetermined attractive and aversive taste behaviors, and substantiate distinct neural substrates for the discrimination of taste identity and the assignment of valence.

The taste system is responsible for detecting and responding to the five basic taste qualities: sweet, sour, bitter, salty and umami[1,2]. Each of these five tastes is detected by specialized taste receptor cells (TRCs) on the tongue and palate epithelium, with different TRCs dedicated to each of the taste modalities[1,2]. In rodents, taste information travels from taste receptor cells in the oral cavity to primary gustatory cortex (insular cortex) via four neural stations[1,3]: TRCs to taste ganglia, then to nucleus of the solitary tract, the parabrachial nucleus, the thalamus, and to insular cortex. Intrinsic[4,5] and 2-photon[6] imaging studies have shown that sweet and bitter taste are represented in the cortex in topographically separate cortical fields; by optogenetically activating these taste cortical fields in awake mice, it is possible to evoke prototypical taste behaviors in the total absence of taste stimuli[7].

The two most important sensory features of a taste stimulus are its identity and its valence. We anticipated that by examining the neural targets of the sweet and bitter cortical fields it may be possible to uncover the circuit logic for appetitive versus aversive tastes. To trace the projections of neurons in sweet and bitter cortex, we labeled neurons in the sweet cortical field with enhanced green fluorescent protein (eGFP), those in the bitter cortex with red fluorescent protein (tdTomato), and then whole brains were examined by clearing and rapid 3D imaging with light-sheet microscopy using CUBIC[8]. Our results showed that projections from the sweet and bitter cortical fields target multiple brain areas, including contralateral taste cortex, amygdala, entorhinal cortex, caudoputamen, and thalamus (see Fig. 1). Most noticeably, sweet and bitter cortical projections exhibited strong segregation as "separate lines" while navigating to the amygdala (Fig. 1b, c; Extended Data Fig. 1), with neurons from the sweet cortical field terminating in the anterior basolateral amygdala (BLAa), while neurons in the bitter cortical field projected predominantly to central amygdala (CEA), with some terminals in posterior BLA. We extended these findings by performing anterograde labeling experiments using Adeno-Associated Virus (AAV)-based trans-synaptic transfer of Cre-recombinase[9] from sweet and bitter cortex to targets in the amygdala. Our results substantiated BLA as the target of sweet cortex projections, and CEA as the target of bitter cortex projections (Fig. 2; see Extended Data Fig. 2 for activity-dependent labeling).

The amygdala is a key brain structure involved in processing emotions, motivation, and positive and negative stimuli[10–19]. Previous studies showed that BLA and CEA both contain distinct populations of neurons that are activated by negative or positive stimuli[10,13–19]. Our finding of such strong segregation of appetitive (sweet) versus aversive (bitter) projections to the amygdala immediately suggests an anatomical division for the generation of valence-specific behavioral responses to tastants.

If the amygdala imposes valence to tastants (i.e. it represents the hedonic value of a tastant to drive valence-specific behaviors), then optogenetic activation of the terminals of sweet cortical neurons in the BLA should elicit attractive responses, while activation of bitter projections should evoke aversive behaviors. Therefore, we generated mice expressing channelrhodopsin-2 (ChR2)[20] in either the sweet or bitter cortical field, implanted optical fibers over the amygdala, and used a place-preference test to measure responses to photostimulation of the cortico-amygdalar projections. Our results (Extended Data Fig. 3), showed that animals avoid the chamber linked to photostimulation of the bitter cortico-

amygdalar projections, but exhibit strong preference for the chamber associated with stimulation of the sweet projections.

Next, we reasoned that optogenetic activation of the terminals of sweet cortical neurons in BLA should trigger appetitive taste behaviors, whereas stimulation of the projections from bitter cortical neurons in CEA should instead impose a negative valence on the stimulus. Thus, we assayed whether ChR2-activation of sweet-to-BLA projections while an animal is drinking a neutral stimulus (e.g. water) transforms it into a highly attractive one like sugar, and conversely, if activation of the projections from bitter cortex to CEA trigger strong laser-dependent suppression of licking, much like introduction of a bitter chemical would do.

We used a behavioral paradigm where ChR2-expressing animals were assayed for water drinking in a head-restrained setup[7]. In these experiments, the laser shutter was placed under contact-licking operation, hence, the animal has control of its own stimulation during the light on-trials, and only self-stimulation would continue to trigger appetitive responses (i.e. light stimulation on its own does not trigger "licking, or licking-like motor responses; see Methods)[7]. In contrast, an animal would immediately terminate licking if contact-licking elicited aversion. Our results demonstrated that optogenetic activation of the sweet cortex terminals in BLA evoked dramatic increase in licking (i.e. self-stimulation; Fig. 3b, c), while activation of the bitter cortical projections to amygdala strongly suppressed licking responses (Fig. 3b, d). To confirm that these light-triggered behaviors were not caused by back-propagation of action potentials from the stimulation in the amygdala (i.e. back to the taste cortex and thus to other potential taste cortical targets), we repeated the experiment, but this time we pharmacologically silenced synaptic activity locally in the amygdala by infusion of the AMPA receptor antagonist NBQX[21]. Our results (Fig. 3e, f) demonstrated that silencing synaptic transmission in the amygdala abolished all light-evoked responses. Importantly, responses fully recovered after washout of the drug (Fig. 3e, f). Taken together, these results demonstrate that activation of sweet or bitter cortico-amygdalar pathways is sufficient to impose a positive or a negative valence on a neutral taste cue.

We hypothesized that strong activation of the bitter- and sweet cortico-amygdalar projections might override the hedonic response elicited by sweet and bitter tastants. Therefore, we predicted that optogenetic activation of the bitter cortical terminals in CEA may impose an aversive response to an orally applied sweet tastant, while strong light stimulation of sweet terminals in BLA might suppress aversion to an orally applied bitter. We used a behavioral test where thirsty animals expressing ChR2 in bitter or sweet cortex were exposed to random presentations of water, a bitter chemical or a sweet solution (Fig. 4a). Next, we examined the impact of photoactivating bitter cortico-amygdalar projections by placing the stimulating optical fiber over the amygdala of the animals expressing ChR2 in bitter taste cortex (Fig. 4b). Figure 4c demonstrates that stimulation of bitter targets in amygdala is indeed sufficient to transform the appetitive nature of a sweet tastant into an aversive one. Conversely, by photoactivating the amygdala targets of sweet taste cortex it was possible to change the perceived valence of a bitter tastant (Fig. 4d, e). These results highlight the key role of the amygdala in imposing valence to a taste cue. To examine the effect of taste stimulation in the absence of amygdala function, we carried out a number of amygdala silencing studies.

First, we used a behavioral assay that relies on direct stimulation of taste cortex. In one group of animals, we introduced ChR2 into neurons in the sweet cortical field (Fig. 5a), bilaterally injected an AAV encoding inhibitory DREADD receptors into amygdala neurons for chemogenetic silencing[22] (see methods for details), and tested the animals before and after clozapine N-oxide (CNO) injection. Importantly, ChR2 and the stimulating fiber are both in sweet cortex (Fig. 5a), and since sweet neurons project to many targets (see Fig. 1a), the full repertoire is likely to be co-activated upon stimulation of the sweet cortical field. Remarkably, silencing the amygdala is sufficient to abolish all attractive responses associated with activation of sweet cortex (Fig. 5b); equivalent results were obtained using pharmacological inhibition of amygdala with NBQX rather than inhibitory DREADD (Fig. 5c). We repeated similar studies but this time examined activation of bitter cortex (Fig. 5d). Our results showed that silencing amygdala is also sufficient to abolish aversive responses associated with activation of bitter cortex (Fig. 5e, f). Finally, we reasoned that the valence associated with sweet and bitter tastants delivered to the tongue, rather than direct stimulation of taste cortex, should also be compromised. As predicted, the results shown in Fig. 5g-i demonstrate that silencing the amygdala dramatically impairs the behavioral attraction or aversion to sweet and bitter chemicals.

Previously, we showed that silencing the sweet or bitter cortex prevented the recognition of sweet or bitter tastants, while optogenetic activation of those same cortical fields triggered prototypical sweet- and bitter-associated behaviors[7]. We reasoned that if tastant identity and valence are encoded in separate neural substrates, with taste cortex responsible for imposing identity to a tastant, and the amygdala for affording its valence, then animals with silenced amygdala should still recognize the identity of a sweet or bitter taste stimulus, even if blind to its hedonic value.

We trained mice to report the identity of a tastant by using two different behavioral assays: a three-port test and a Go/No-go assay. In the three-port test, mice learned to sample a taste cue from a center spout (random presentations of water, a sweet or a bitter chemical), and then report its identity either by going to the right or left port; a correct response was rewarded with 4 seconds of water (Fig. 6a). We initially focused on attractive responses as they represent the expression of a selective, positive behavioral response. After 20–30 sessions of training over 10–14 days (see Methods for details), trained mice: (1) were able to report the identity of each tastant in hundreds of randomized trials with over 90% accuracy (see for example Fig. 6b); (2) properly cross-generalized to other sweet and bitter tastants (not used in the training set) with the correct behavioral response (Fig. 6b, compare training to testing), and (3) appropriately reported direct optogenetic activation of sweet taste cortex as "sweet", with ~90% of the water + light trials producing correct responses (Fig. 6c, "Pre" silencing; see also Ref 7). Next, we assayed whether silencing amygdala via inhibitory DREADD to BLA affected the ability of these animals to correctly identify a sweet stimulus. Our results (Fig. 6c) demonstrated that loss of amygdala function, while abolishing the ability of sweet cortex to evoke appetitive responses (see Fig. 5a-c), has no impact on the ability of the animals to properly identify sweet tastants (or to recognize light-activation of sweet cortex as "sweet"). As anticipated, inhibitory DREADD expression in sweet cortex (just as previously shown using NBQX[7]), severely impairs sweet taste recognition (Extended Data Fig. 6).

The second behavioral platform relied on Go/No-go behavioral assays, and examined both sweet and bitter recognition. Thirsty animals were trained to sample a test tastant from a spout, and then to report its identity either by licking (go) or withholding licking (no-go; Fig. 6d). We trained animals to go to bitter and no-go to sweet, exactly the opposite of the innate drive. After 15–20 sessions of training, mice reported tastant identity with over 90% accuracy (Fig. 6e). Our results (Fig. 6f) showed that silencing the amygdala, just as observed in the 3-port tests, indeed has no effect on recognition of sweet or bitter tastants. Importantly, these experiments used the same animals that exhibited strong loss of sweet and bitter valence after NBQX infusion to the amygdala (Fig. 5g-i). Taken together, these studies substantiate the amygdala as necessary and sufficient to drive valence-specific behaviors to taste stimuli, and the cortex to independently represent taste identity.

The senses of taste and smell function as the principal gateways for assessing the attraction to, and palatability of food cues. In its most fundamental state, taste mediates innate consummatory and rejection behaviors, while also allowing an animal to learn the association of food sources with hardwired tastant-dependent actions. Here we studied the neural basis for innate responses to sweet and bitter, and showed that taste cortex and the amygdala function as two essential, but distinct neural stations for identifying tastants and for imposing valence to sweet and bitter.

Recent molecular studies have identified distinct populations of neurons in amygdala that may serve as neural substrates for a wide range of positive and negative hedonic responses[10,13–19]. In this study, we showed that sweet and bitter cortical fields exhibit separate projection targets in amygdala, and that photoactivation of these cortico-amygdalar projections evokes opposing responses. Most interestingly, however, these can be experimentally dissociated from cortex, such that animals may recognize a "taste stimulus" but remain oblivious to its valence. Together, these results provide an anatomical substrate for imposing hedonic value to sweet and bitter, and the basic logic for the generation of hardwired, stereotyped attractive and aversive taste responses.

The amygdala is known to provide representations of Pavlovian associations[11,23,24], such that innately rewarding and aversive tastants may also function as unconditioned stimuli in conditioning protocols[25]. Therefore, in addition to imposing valence on tastants, the amygdala likely links taste valence to other stimuli so that associative memories can be formed, and thereby appropriate valence-specific behavior may be elicited by previously neutral cues from other modalities that would now predict a bitter or sweet tastant. Notably, sweet and bitter cortex project to several additional brain areas, including those involved in feeding, motor systems, multisensory integration, learning and memory (Fig. 1). In the future, it will be exciting to unravel how these circuits come together to drive innate and learned responses.

Online Methods

Animals and Surgery procedures

All procedures were carried out in accordance with the U.S. National Institutes of Health (NIH) guidelines for the care and use of laboratory animals, and were approved by the

Columbia University Institutional Animal Care and Use Committee. Seven- to nine-week-old male C57BL/6J mice and B6.Cg-Gt(ROSA)26Sor[tm9(CAG-tdTomato)Hze]/J mice (Ai9)[30] were used for viral injections.

Animals were anesthetized with ketamine and xylazine (100 mg/kg and 10 mg/kg, intraperitoneal), placed into a stereotaxic frame with a close-loop heating system to maintain body temperature, and unilaterally injected with 20–50 nl of AAV carrying ChR2 (AAV9.CamKIIa.hChR2(H134R)-EYFP.WPRE.SV40, Penn Vector Core) either in the sweet cortical field (bregma 1.7 mm; lateral 3.1 mm; ventral 1.8 mm) or the bitter cortical field (bregma −0.35 mm; lateral 4.2 mm; ventral 2.7 mm). The location of the taste cortex was verified by anatomical and optogenetic assays. Anterograde tracing[6] and retrograde tracing (Extended Data Fig. 7) showed these cortical areas receives input from taste thalamus (VPMpc). Photostimulation of these sweet and bitter cortical fields evokes prototypical attractive and aversive taste behaviors, respectively[7]. We also examined behavioral data from 14 ChR2 injections in the middle (Extended Data Fig. 8); six of the animals showed modest increase in lick responses, 3 exhibited no change, and 5 showed a small range of aversion. We believe this variability likely reflects the spread of the injection site.

Following viral injections, a customized implantable fiber (Core diameter 200 μm, NA 0.39) was implanted 300–500 μm above the injection site, and guide cannulas (26 gauge, PlasticsOne) were unilaterally or bilaterally implanted above anterior BLA (bregma −1.0 mm; lateral 3.2 mm; ventral 3.7 mm) or CEA (bregma −1.2 mm; lateral 3.0 mm; ventral 3.7 mm). These guide cannulas were used both for photostimulation of cortical projections and intracranial infusion in pharmacological silencing experiments. A metal head-post was attached for head fixation during behavioral tests. All implants were secured onto the skull with dental cement (Lang Dental Manufacturing). For chemogenetic silencing experiments, 150–250 nl of AAV carrying hM4Di (AAV8.hSyn.hM4Di–mCherry, UNC Vector Core) was injected bilaterally into BLA (bregma −1.0 mm; lateral 3.2 mm; ventral 4.2 mm) or sweet cortical field (bregma 1.7 mm; lateral 3.1 mm; ventral 1.8 mm) at a slow rate (15 nl/min). All ventral coordinates listed above are relative to the pial surface. Mice were allowed to recover for at least 2–3 weeks before the start of behavioral experiments. For anterograde transsynaptic tracing, AAV1.hSyn.Cre[9] (20–50 nl) was injected into the sweet- or bitter cortical field of animals carrying a Cre-dependent tdTomato reporter (Ai9[30]). Animals were examined 4 weeks after the injection. Placements of viral injections, guide cannulas, and implanted fibers were histologically verified at the termination of the experiments using DAPI (1:5000, Thermo Fisher Scientific) or TO-PRO-3 (1:1,000, Thermo Fisher Scientific) staining of 100 μm coronal sections. A confocal microscope (FV1000, Olympus) was used for fluorescence imaging.

Whole-brain clearing and imaging

For whole-brain tracing of the projections of cortical neurons, we unilaterally injected with a small volume (10–20 nl) of mixed AAVs carrying Cre recombinase and Cre-dependent eGFP (AAV1.CamKII0.4.Cre.SV40 and AAV1.CAG.Flex.eGFP.WPRE.bGH, 1:100, Penn Vector Core) in the sweet cortical field, and the same volume of mixed AAVs carrying Cre recombinase and Cre-dependent tdTomato (AAV1.CamKII0.4.Cre.SV40 and

AAV9.CAG.Flex.tdTomato.WPRE.bGH, 1:100, Penn Vector Core) in the bitter cortical field. Four weeks after AAV injection, mice were transcardially perfused with 5–10 ml of phosphate buffered saline (PBS) containing 10 U/ml heparin, followed by 20 ml of 4% paraformaldehyde; brains were post-fixed in 4% paraformaldehyde for an additional 3 hours at room temperature. Whole brains were then treated following the CUBIC clearing protocol[8,31]. To prevent sample deformation caused by temperature fluctuation and to minimize fluorescence loss during clearing, all clearing procedures were performed at room temperature. CUBIC clearing reagents were prepared as previously described[8,31]. Reagent-1 contained 25 wt% urea (Sigma-Aldrich), 25 wt% *N,N,N',N'*-tetrakis (2-hydroxypropyl) ethylenediamine (Sigma-Aldrich), and 15 wt% Triton X-100 (Nacalai Tesque). Reagent-2 contained 50 wt% sucrose (Sigma-Aldrich), 25 wt% urea, 10 wt% triethanolamine (Sigma-Aldrich), and 0.1% (v/v) Triton X-100. The fixed brains were washed three times with PBS, immersed in reagent-1 (diluted 1:2 in water) overnight with gentle shaking and then incubated in reagent-1 for 7–10 days with gentle shaking. Brains were washed with PBS, degassed in PBS overnight and were then transferred into 5 ml of reagent-2 diluted 1:2 in PBS for 6–24 hours before immersion in reagent-2 for 3–7 days for further clearing and reflection index matching. TO-PRO-3 (1:5,000, Thermo Fisher Scientific) was added to reagent-2 for counterstaining. During the immersion in reagent-2, tubes were not shaken to avoid bubbles. Samples were kept in reagent-2 for up to 1 week at room temperature before imaging.

On the day of imaging, samples were gently wiped to remove reagent-2 residue and transferred into an oil mix (mineral oil and silicone oil 1:1, final refraction index 1.48–1.49) at least 1hr before imaging. Light-sheet fluorescence microscopy (UltraMicroscope, LaVision BioTec) with a 2x objective lens (NA 0.5, working distance 10 mm) or 4x objective lens (NA 0.3, working distance 6 mm) was used for rapid image acquisition of the whole brain. The samples were sequentially illuminated with a unidirectional light-sheet produced by 488 nm, 561 nm and 640 nm lasers and scanned with a z-step size of 8.13 – 13 μm from ventral to dorsal. Exposure time was 50 – 200 ms per channel per z-step. To cover the whole brain, each sample was imaged either via 4×4 tile-scan with 4x lens or using multi-position scan with 2x lens (three manually assigned positions to cover two hemispheres and brainstem).

Whole-brain image tiles were scaled to 1/8 of the original size and stitched in three dimensions using ImageJ 1.51n (Fiji distribution). The 640 nm channel of the whole-brain data was registered to a reference atlas (Allen Brain Institute, 25 μm resolution volumetric data with annotation map, http://www.brain-map.org) using ANTs (Advanced Normalization Tools 1.9.x) with affine transformation[26,32]. The same transformation was applied to the other two channels using the *WarpImageMultiTransform* function of ANTs. Z-projections of maximum intensity and virtual sections were processed in ImageJ (noise was filtered with the remove outlier function). Because of the high dynamic range of the fluorescent intensity between the soma and the fine processes, the gamma value of the images shown in Fig. 1 was set to 0.5 for display purposes.

c-Fos induction and immunohistochemistry

Mice expressing ChR2 in the sweet- or bitter cortex were habituated by performing mock stimulations (see below) once a day for 3 days prior to c-Fos induction. On the day of the experiment, animals were photostimulated for 30 min (473 nm, 20 Hz, 20-ms pulses, 5 s on and 5 s off, 5–10 mW/mm^2). Mice were then allowed to rest for 1 hour and were processed for immunostaining as previously described[7]. Tissue sections were incubated with goat anti-c-Fos antibody (1:500, Santa Cruz, sc-52-G) for 24 hours at 4 °C. Fluorescent tagged-secondary antibodies (Alexa-594 donkey anti-goat or Alexa-647 donkey anti-goat, 1:1000, Thermo Fisher Scientific) were used to visualize c-Fos expression. All sections were imaged using an Olympus FV-1000 confocal microscope.

Head-restrained lick preference assays

Head-restrained lick preference assays were performed as previously described[7]. Mice expressing ChR2 in sweet or bitter cortex were initially water-deprived for 24 hours to motivate drinking in head-restrained assays and then acclimated to drinking from a motor-positioned spout (two sessions per day for at least 2 days) before testing. Mice were weighed daily during the behavioral assays and supplied with necessary water to maintain at least 85% of their initial body weight. Each trial began with a light cue, followed 1 s later by the spout swinging into position and a tone cue to indicate the onset of tastant delivery; after 5 s (during which the animal could lick) the spout rotated out of position. To measure attractive responses, mice were mildly water restricted (water-deprived for 24 hours, and then provided with water until they exhibited an average of 5–15 licks per 5 seconds window); mice were supplied with 2–5 μl water at the beginning of each trial. To measure aversion, mice were water-deprived for 24 hours, and supplied with 5–10μl water per trial; mice normally exhibited active licking over the full five seconds (average 30–40 licks per 5 seconds as a sign of thirst). Training sessions consisted of 60 trials of water; testing sessions shown in Fig. 3 consisted of 15 trials of water, 4 of which coupled to photostimulation of cortical terminals in the amygdala; testing sessions in Fig. 5b-f consisted of 20 trials of water, 10 of which pseudo-randomly coupled to photostimulation of sweet cortex; testing sessions in Fig. 4 consisted of 60 trials, 20 trials of water, 20 trials of bitter (0.5mM quinine), 20 trials of sweet (4mM AceK). To examine the effect of amygdalar nuclei on taste preference, 50% of sweet trials in Fig. 4c or 50% of bitter trials in Fig. 4e were pseudo-randomly coupled to photostimulation of CEA (Fig. 4c) or BLA (Fig. 4e). The delivery of tastants was triggered by licking action such that mice could consume as much or little as they chose during the 5 seconds. To minimize the influence of thirst and satiety on assessment of taste palatability, for each test-session in Fig. 4 we included consecutive trials satisfying two criteria: 1) licks to bitter less than 20 (otherwise mice were too thirsty); 2) more than 5 licks to water (otherwise mice were already satiated). The licking behavior was videotaped during the entire session and licking events were identified by a custom-MATLAB program. For photostimulation, 473nm light stimuli (diode-pumped solid-state laser, Shanghai Laser & Optics Century Co. or fiber-coupled LED, Thorlabs) were delivered via an optical fiber inserted into a guide cannula over the amygdala or via an implantable fiber over taste cortex. Light stimulation was controlled by contact of the tongue with the metal spout; one lick triggered a train of light pulses (10–20 Hz, 20 ms per pulse, 20 pulses, 5–15 mW/mm^2). Licks during the light stimulation extended the stimulus until 1 second

after the last lick. Light / tone cues, the delivery of tastants and light stimuli were controlled using a MATLAB program via a microcontroller board (Arduino Mega 2560, Arduino)[7]. Each point in Fig. 3c-f and Fig. 4 indicates data averaged from multiple test sessions for an individual mouse. In Fig. 3e-f, lick ratio refers to the number of licks in the presence of light stimulation over the number of licks in water-only trials.

Free-moving lick preference assays

Taste preference (Fig. 5 g-i) was also measured in free-moving animals by using a custom-built gustometer[33]. Prior to testing, mice were water restricted for 24 hours, and then provided with water until they exhibited an average of < 20 licks per 5 seconds window (to test attractive responses). Alternatively, after 24 hours of water restriction mice were provided with unrestricted water access for 5–10 min, and then assayed 18 hours later (i.e. to test aversive responses animals need to be sufficiently thirsty to be motivated to sample an unattractive cue). For testing, mice were presented with water vs. 4mM AceK or water vs. 1mM quinine as previously described[33].

Place preference assays

Mice expressing ChR2 in sweet- or bitter cortex were tested in a custom-built two- chamber arena placed inside a sound attenuating cubicle; the arena (30 cm×15 cm), was designed with one chamber with alternating black and white vertical stripes, and the other with alternating black and white squares. Animal locations were tracked in real-time by videotaping[7]. Mice were tested in the arena for 30 min with photostimulation of the sweet- or bitter cortico-amygdalar projections via an optical fiber above BLA or CEA, respectively. The last 15 min of each testing session were used to calculate the preference index (PI); $PI = (t_1 - t_2)/(t_1 + t_2)$, where t_1 is the fractional time a mouse spent in the chamber 1 (stimulating chamber), and t_2 is the time spent in chamber 2 (non-stimulating chamber). For photostimulation of the sweet cortico-amygdalar projections, light was delivered for 5 s, with a 3-s interval (20 Hz, 20-ms pulses, 5–10 mW/mm^2) to avoid over-stimulation or phototoxicity; for photostimulation of the bitter cortico-amygdalar projection, light (20 Hz, 20-ms pulses, 2–5 mW/mm^2) was delivered for 1 s with a 3-s interval; a sound cue was used to mark the onset of each stimulation[15,34,35]. For each cohort (8 mice for sweet and 5 animals for bitter), half the animals were tested with light on the baseline-preferred chamber, and half with light on the baseline unpreferred chamber[15,34]. When the animal crossed to the non-stimulating chamber, the light was automatically turned off immediately.

Three-port taste recognition assays

Mice deprived of water for 24 hours were trained to perform a taste recognition task in a customized three-port behavior chamber in which they sampled taste cues from the middle port and then reported the taste identity of the cue by choosing to lick from either the left or right port. Taste cues (AceK, quinine or water) were pseudo-randomly delivered through a metal spout in the middle port. Each trial began with the shutter opening in the middle port. Mice were given (up to) 15 s to initiate a trial by licking the middle spout (failure to initiate a trial resulted in the shutter closing and a new trial starting). The shutter in the middle port closed 0.5 s after the first lick allowing animals 0.5 s to sample tastants cues (2–3 μl); 0.5 s after the middle port closed, the shutters of the left and right ports opened simultaneously.

Mice were given 4 s to make a left or right choice and obtain water reward (total ~6 μl). For a given mouse, reward from side ports was assigned to taste cues (e.g. left for sweet, right for bitter and water). A wrong choice triggered a penalty of a 5 s timeout. The inter-trial interval was 1 s. Mice were trained for two sessions per day, with 80–100 pseudo-randomized trials per session until they could effectively discriminate the tastants with ~90% accuracy (2–3 weeks). To test the effect of photostimulation of sweet cortical neurons, mice expressing ChR2 in sweet cortex were trained to discriminate sweet from bitter and water (e.g. left for sweet, right for either bitter or water) and then tested with sweet, bitter, water, and water + light (473nm, 20 Hz, 20 ms per pulse, 20 pulses triggered by one lick of middle spout). A testing session consisted of 20 sweet trials, 20 bitter trials, 10 water-only trials and 10 water + light trials. To avoid mice using photostimulation light as a visual cue, the connection between implantable fiber and patch cable was properly shielded. To prevent learning during the test, no time out penalties were given and no reward was provided for water + light trials. Performances were calculated as the percentage of correct choice for a given taste cue. The lick behavior was detected by a capacitive touch sensor (MPR121, SparkFun). The delivery of tastants, shutter position and light stimuli were controlled by a custom-MATLAB program via an Arduino board.

Go/No-go taste recognition assays

Go/No-go taste recognition assays were performed as previously described[7]. Mice were trained until they could effectively discriminate the tastants with ~90% accuracy (over 1–2 weeks). On the 'probe' sessions, no punishment was applied for 'no-go' tastants to avoid re-learning; neither reward nor punishment were delivered to novel tastants.

Pharmacological inhibition

The selective AMPA receptor antagonist NBQX (5 mg/ml in 0.9% NaCl, 100–300 nl, Tocris Bioscience) was unilaterally (Fig. 3e-f) or bilaterally (Figs. 5 and 6) infused into the amygdala using a 1 μl microsyringe (Hamilton) and an internal cannula (PlasticsOne) inserted into the guide cannula above amygdala. The infusion rate was approximately 100 nl/min. After the intracranial infusion, mice were allowed to rest in their home-cage for 1–1.5 hour before re-test. A post-test was performed after a recovery period of 24 hours. As a control, the same experiment was conducted using isotonic saline (0.9% NaCl) in the same animals.

Chemogenetic inhibition

Mice injected with ChR2 in sweet cortex and hM4Di in BLA were first tested in the head-restrained lick preference assay as described above. To effectively examine inhibition using hM4Di, we determined (and used) the minimum light intensity for photostimulation that produced significant attractive responses (pre-test). On the following day, CNO was injected (10 mg/kg, intraperitoneal) and the behavioral test with the same level of photostimulation was repeated between 1 and 2 hours after CNO injection. Mice were allowed to rest and recover in their home cage and a post-test was performed at least 24 hours later.

The same mice were then trained in the three-port assay for taste recognition. After achieving at least 90% accuracy in training sessions, mice were tested for the ability to

recognize tastants and optogenetic stimulation of the sweet cortex in the three-port taste recognition assay before and after chemogenetic silencing (Pre: 24 hours before CNO injection; CNO: between 1–2 hours after injection; Post: at least 24 hours after injection). To confirm that amygdala was indeed efficiently silenced in the experiments presented in Fig. 6c, mice were tested for attractive responses to photostimulation of sweet cortex in a lick preference assay; this was performed after each three-port session before and after chemogenetic silencing.

Statistics

No statistical methods were used to predetermine sample size, and investigators were not blinded to group allocation. No method of randomization was used to determine how animals were allocated to experimental groups. Animals in which post-hoc histological examination showed that viral targeting or the position of implanted fiber / cannulas was in the wrong location were excluded from analysis. Statistical methods are indicated when used, and statistical analyses for all figures are provided in Supplementary Table 1. Multiple comparisons were analyzed using Repeated Measures one-way or two-way ANOVA followed by the Bonferroni correction. All analyses were performed in MATLAB 2016a (MathWorks), Prism 7.0a (GraphPad), and Igor Pro 6.37 (WaveMetrics). Data are presented as mean ± s.e.m.
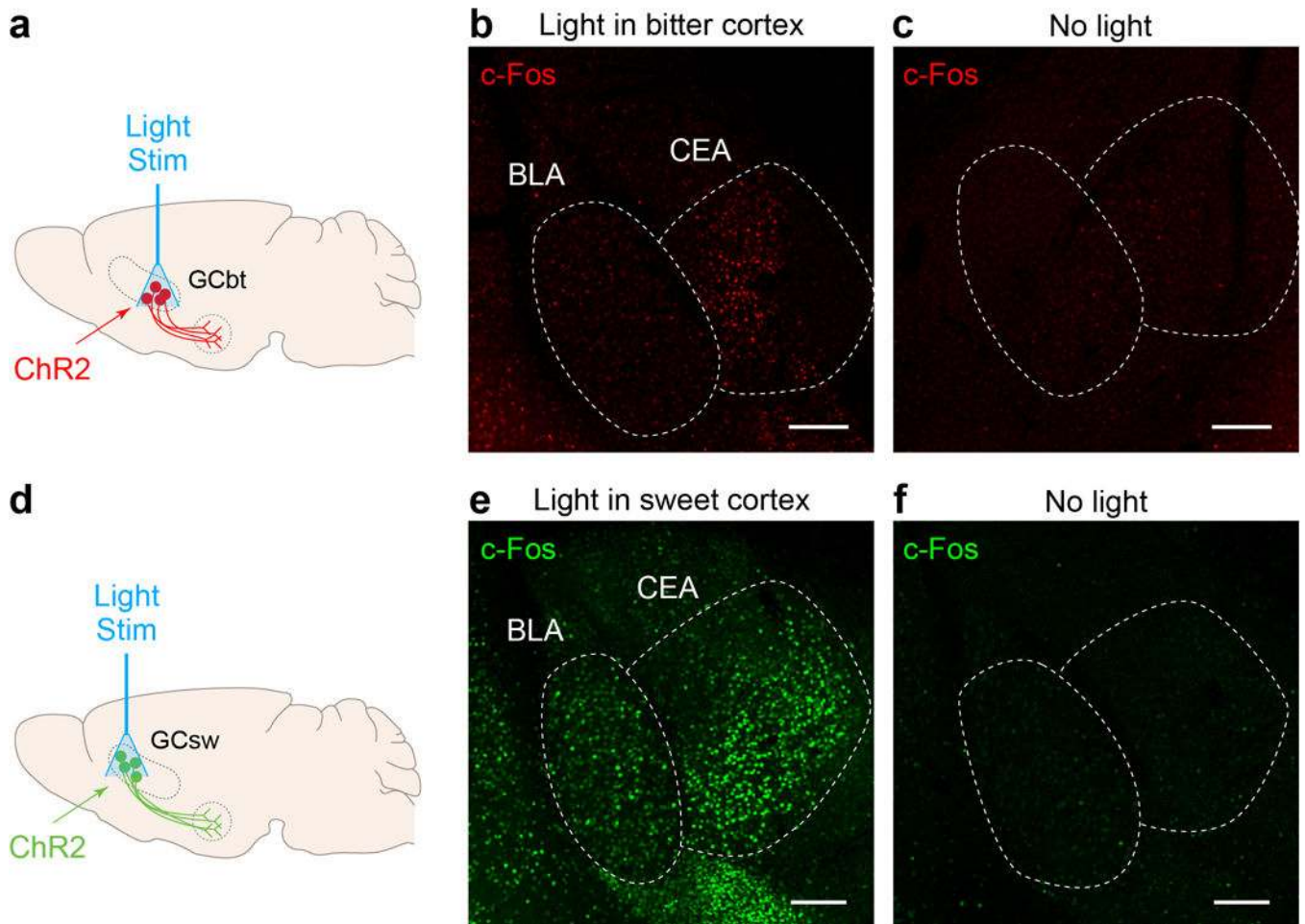
Extended Data
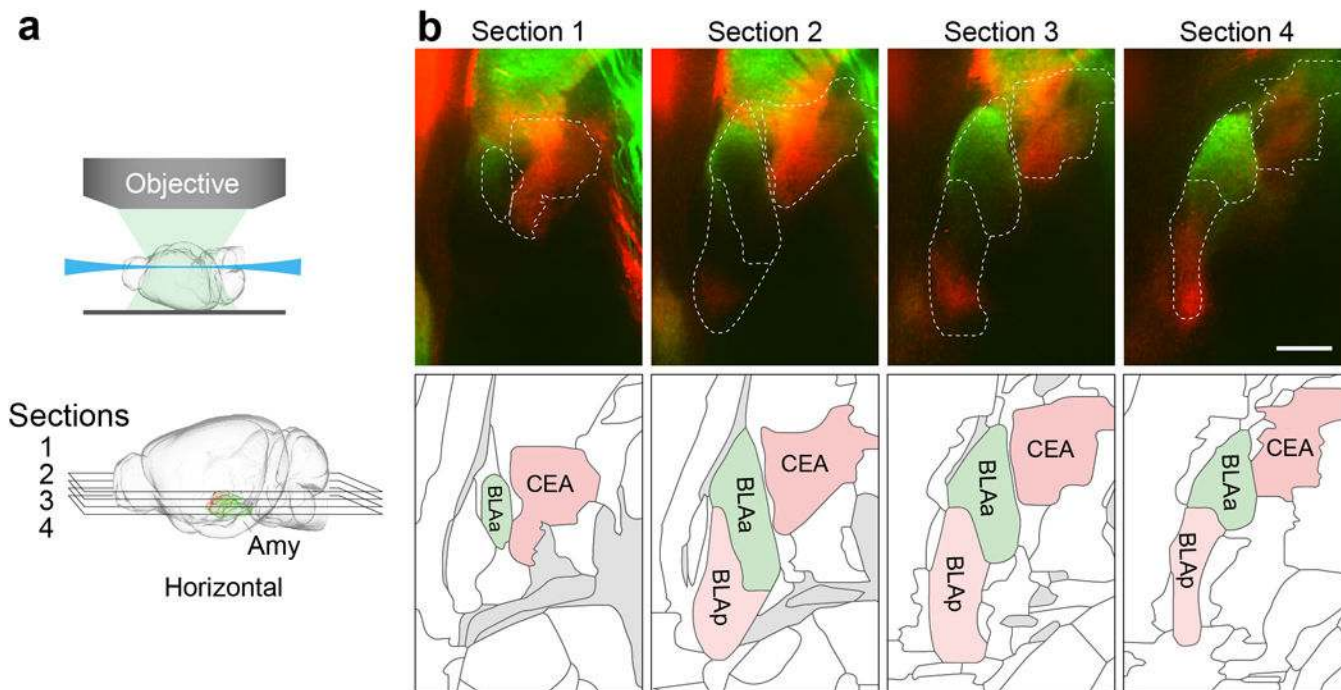
Extended Data Figure 1: Projections from sweet and bitter cortex terminate in distinct targets in the amygdala – Horizontal Sections.
a, The cartoon illustrates the imaging planes with optical horizontal sections at different depths of amygdala (Amy). The brain diagrams were rendered by the Scalable Brain

Composer (https://scalablebrainatlas.incf.org/services/sba-composer.php?
template=ABA_v3) based on Allen Mouse Brain Common Coordinate Framework version
326,27. **b**, Segregation of sweet and bitter cortical projections in amygdala. Sweet cortical
neurons project to anterior basolateral amygdala (BLAa, green), while bitter cortical neurons
predominantly innervate central amygdala (CEA, red), and to a portion of posterior
basolateral amygdala (BLAp, red). Shown are optical horizontal sections at different dorsal-
ventral positions (upper panels, sections 1-4; see panel a). The boundaries of amygdala
nuclei were determined by aligning fluorescence images to the Allen Brain Institute atlas26
(lower panels; http://brain-map.org/). Scale bar, 500 μm. Similar results were observed in 6
independently labeled and imaged animals.

Extended Data Figure 2: Activity-dependent labeling of sweet and bitter cortical targets in the amygdala.
Shown are activity-dependent labeling of sweet and bitter cortical targets in the amygdala by
probing for c-Fos expression[16] in response to optogenetic activation of the sweet and bitter
cortical fields. **a**, Schematic of optogenetic stimulation strategy in bitter cortex for c-Fos
induction. **b**, c-Fos expression in amygdala in response to photostimulation of bitter cortex.
The majority of c-Fos positive neurons are localized to CEA. **c**, c-Fos expression in a control
mouse without light stimulation. **d**,**e**,**f**, Photostimulation of sweet cortex induces c-Fos

expression in amygdala. Note that CEA, as a major local output of BLA[11,36], also shows strong c-Fos labeling in response to photostimulation. Scale bars, 200 μm. Similar results were obtained in 3 animals for each experiment.
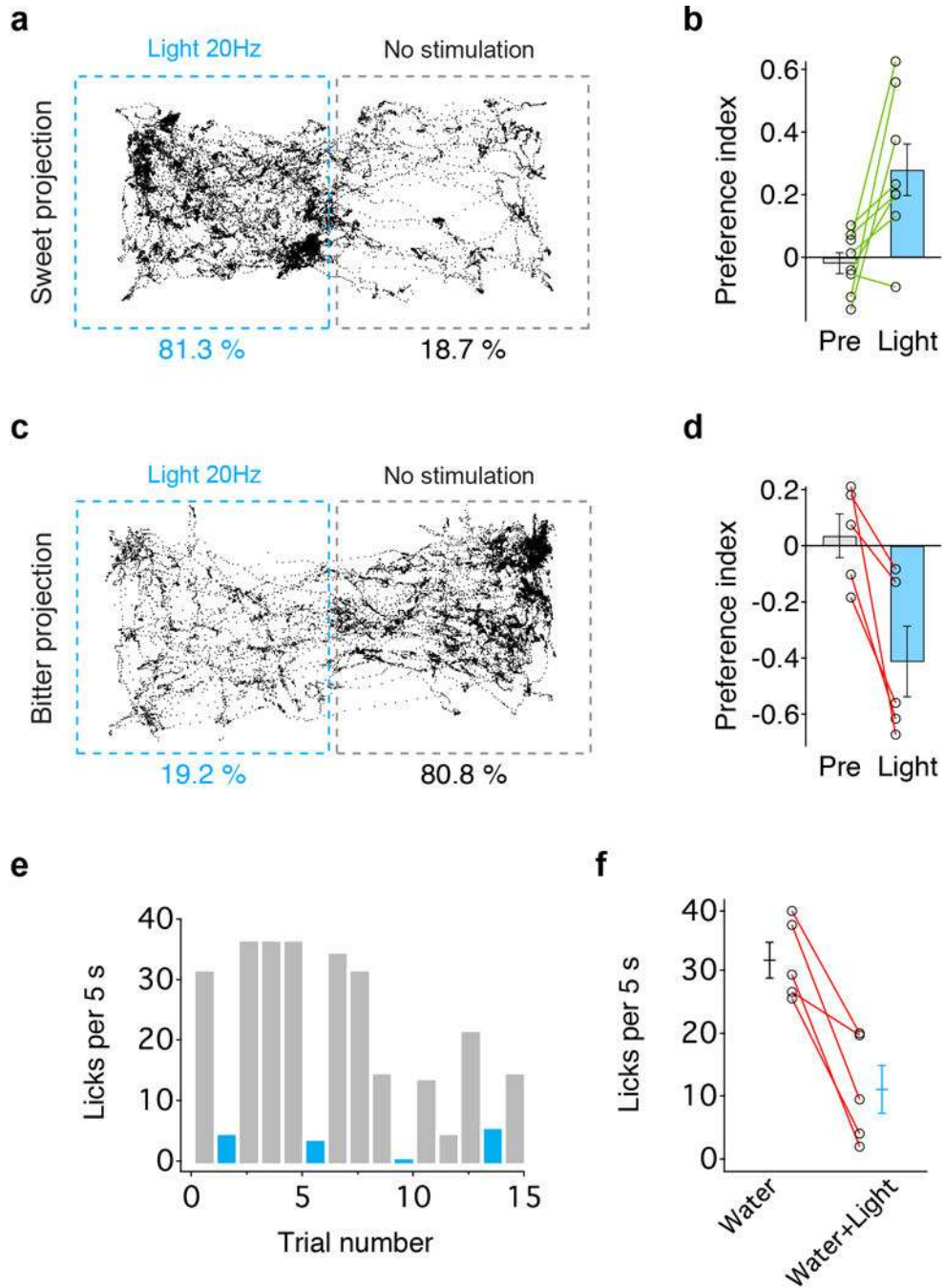

Extended Data Figure 3: Place preference by photostimulation of cortico-amygdalar projections.
a, Representative tracking of a mouse during the 15min place preference test in a two-chamber arena; the left chamber in the diagram was coupled to stimulation of sweet cortico-amygdalar projections (see Methods for details); this animal spent over 80% of the test time

in the chamber linked to stimulation of sweet projections to amygdala. **b**, Quantification of preference index before (Pre) and during light stimulation (n=8 mice, two-tailed paired t-test, P=0.0156). **c, d**, Place preference test with stimulation of bitter cortical projection in amygdala (n=5 mice, two-tailed paired t-test, P= 0.0207). **e, f**, Animals used in panel d were also tested in a licking assay with similar light stimulation intensity, demonstrating strong suppression of licking responses (n=5 mice, two-tailed paired t-test, P=0.0056). Values are mean ± s.e.m. We note that we have examined multiple independent behavioral experiments activating sweet projections to BLA and have never observed the induction of motor patterns, or consummatory behavior. Strong stimulation of bitter cortico-amygdalar projections (20Hz, 10–15 mW) often elicited prototypical orofacial rejection behavior (see Supplementary Video 1).
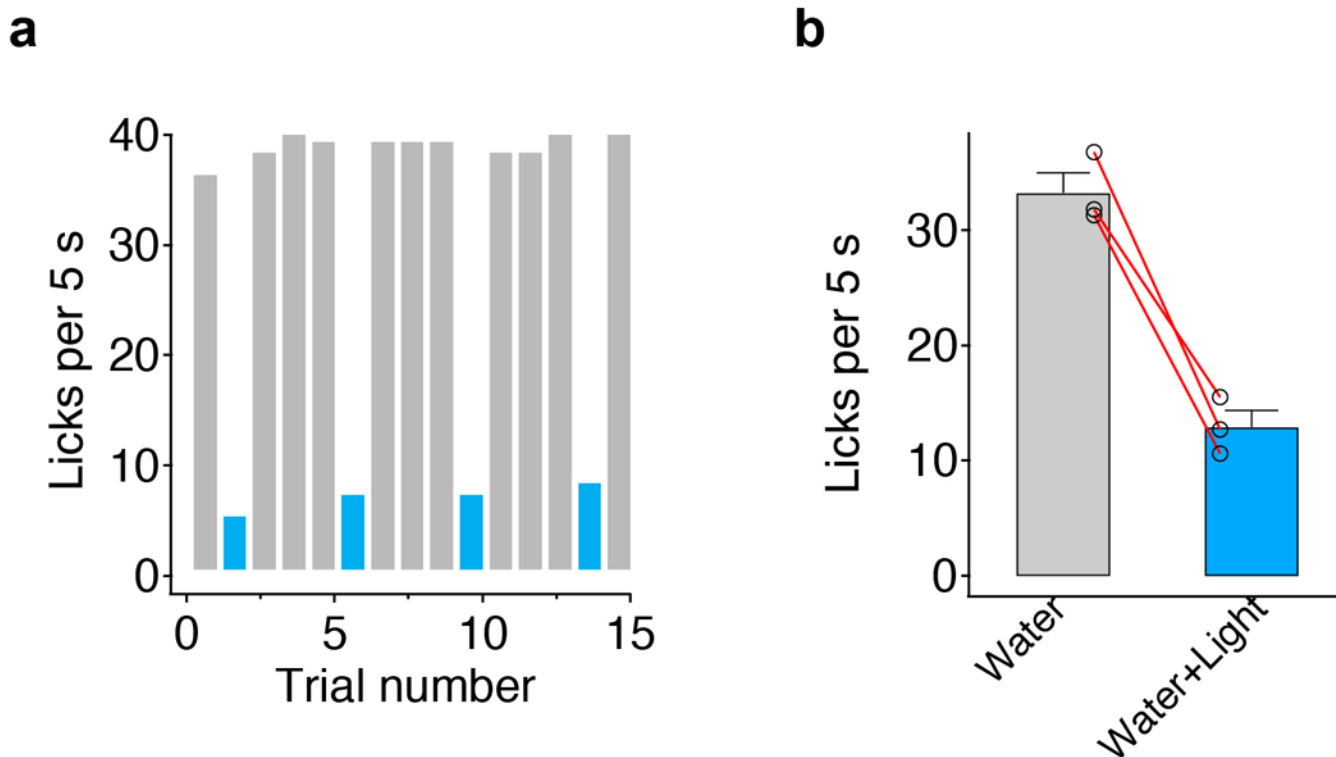

Extended Data Figure 4: Activation of bitter cortical projections to posterior BLA is aversive.
As shown in Figure 1 and Extended Data Fig. 1, a fraction of the bitter cortico-amygdalar projections terminate in posterior BLA (BLAp). As expected, stimulation of these projections elicits aversive responses. **a**, Representative histograms showing licking events in the presence (blue) or absence (grey) of photostimulation of bitter cortical projections to posterior BLA. AAV-ChR2 was injected into bitter cortex, and the stimulating fiber was targeted above posterior BLA (coordinates: bregma −2 mm; lateral 3.4 mm; ventral 4.3 mm). **b**, Quantitation of licking responses (n=3 mice, two-tailed paired t-test, P=0.0121). Values are mean ± s.e.m.
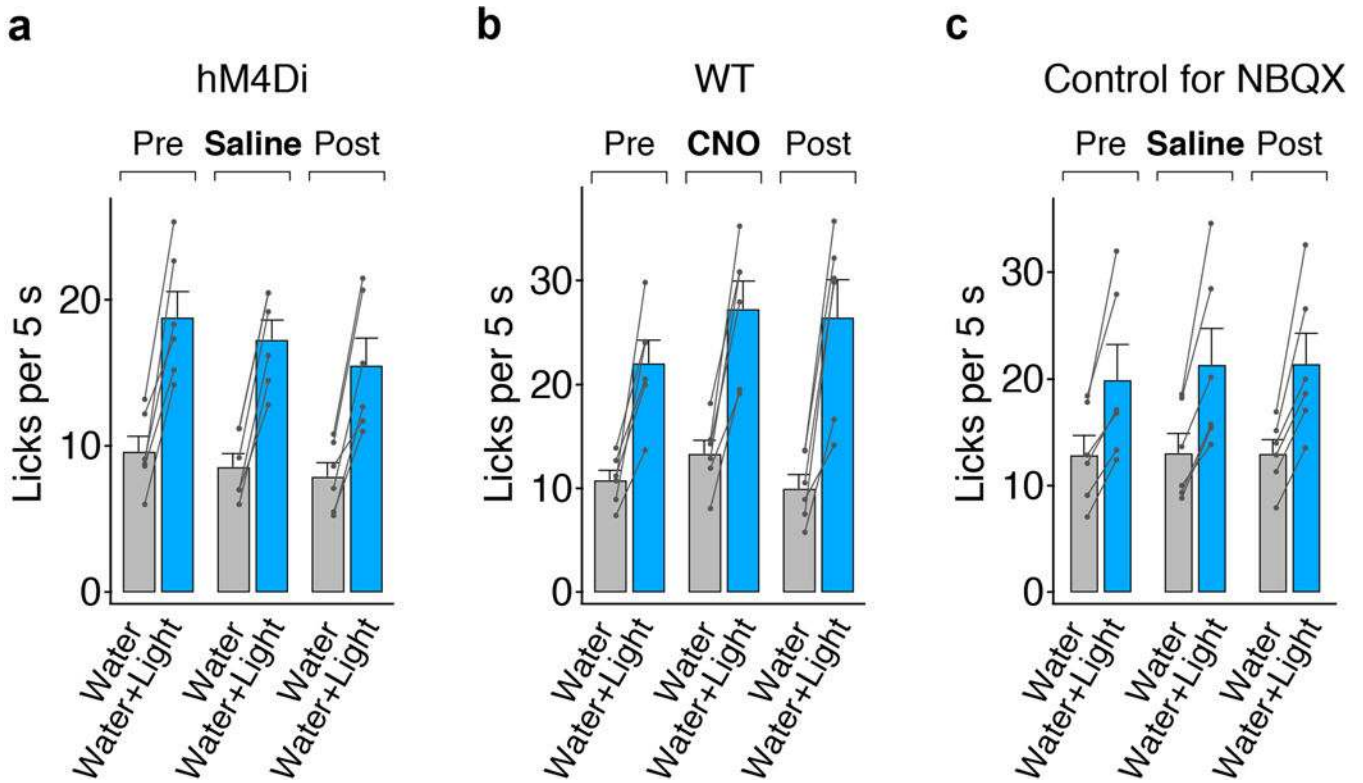
Extended Data Figure 5: Control experiments for silencing amygdala with DREADD and NBQX.

a, Quantification of licking response before and after saline administration in animals expressing inhibitory DREADD (hM4Di; see Fig. 5); n=6 mice, two-tailed paired t-test, Pre: P=0.0011, Saline: P<0.0001, Post: P=0.0014. **b**, Quantification of licking response before and after CNO administration (10 mg/kg) in wildtype animals (WT, non-DREADD expressing); n=6 mice, two-tailed paired t-test, Pre: P=0.0025, CNO: P=0.0008, Post: P=0.0021. **c**, Controls with saline infusion instead of NBQX for Fig. 5c; n=6 mice, two-tailed paired t-test, Pre: P=0.0080, Saline: P=0.0054, Post: P=0.0046. Values are mean ± s.e.m.
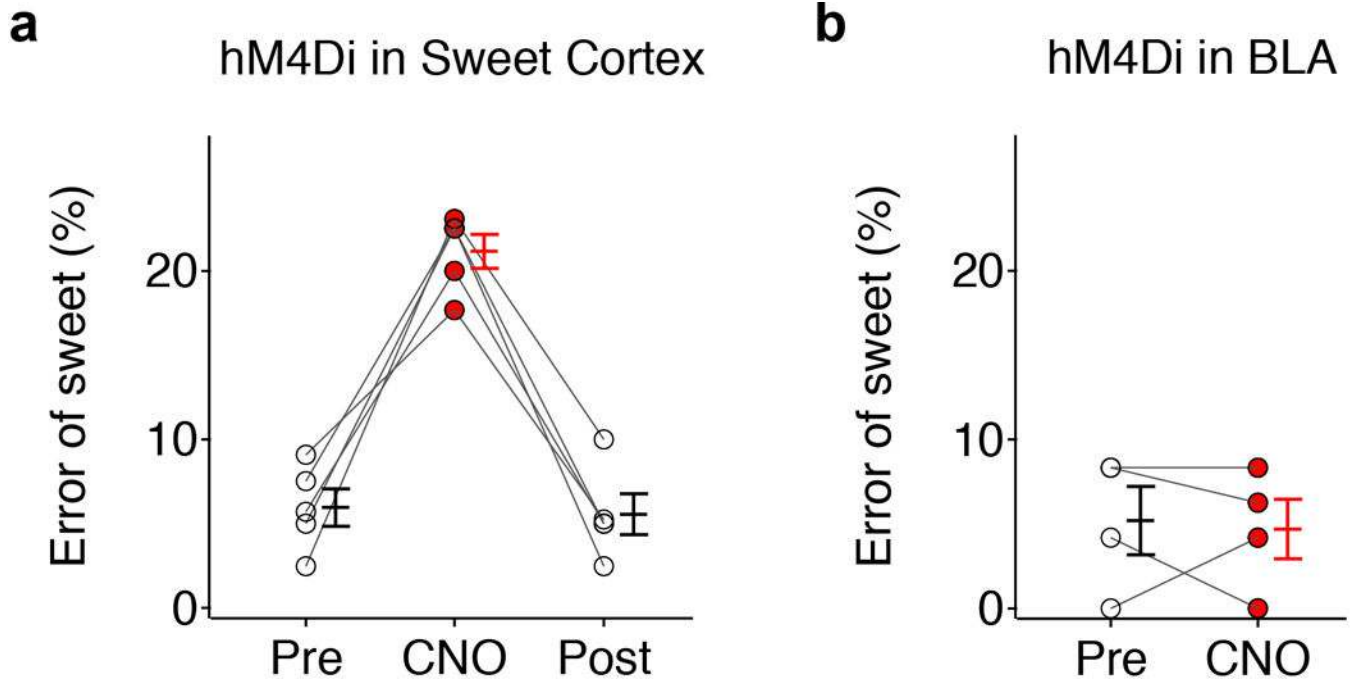
Extended Data Figure 6: Chemogenetic silencing taste cortex impairs tastant recognition.
a, Quantitation of the error rate for sweet taste recognition (2mM AceK) in a three-port assay before and after silencing sweet taste cortex with inhibitory DREADD (hM4Di) and CNO (10 mg/kg); n=5 mice, RM one-way ANOVA followed by Bonferroni post-hoc test, $F_{(2, 8)}$=46.84, P<0.0001. See also Ref 7 for pharmacological silencing with NBQX. **b**, Quantitation of the error rate of sweet taste recognition (1mM AceK) before and after silencing the amygdala with inhibitory DREADD (hM4Di) and CNO (10 mg/kg); n=4 mice, two-tailed paired t-test, Pre vs. CNO: P=0.7888. See also Fig. 6. Note that sweet recognition was only affected by silencing the taste cortex, but not the amygdala. All animals tested recognized sweet taste with the correct behavioral choice (prior to silencing) in at least 90% of the trials. Values are mean ± s.e.m. See Supplementary Table 1 for detailed statistics.
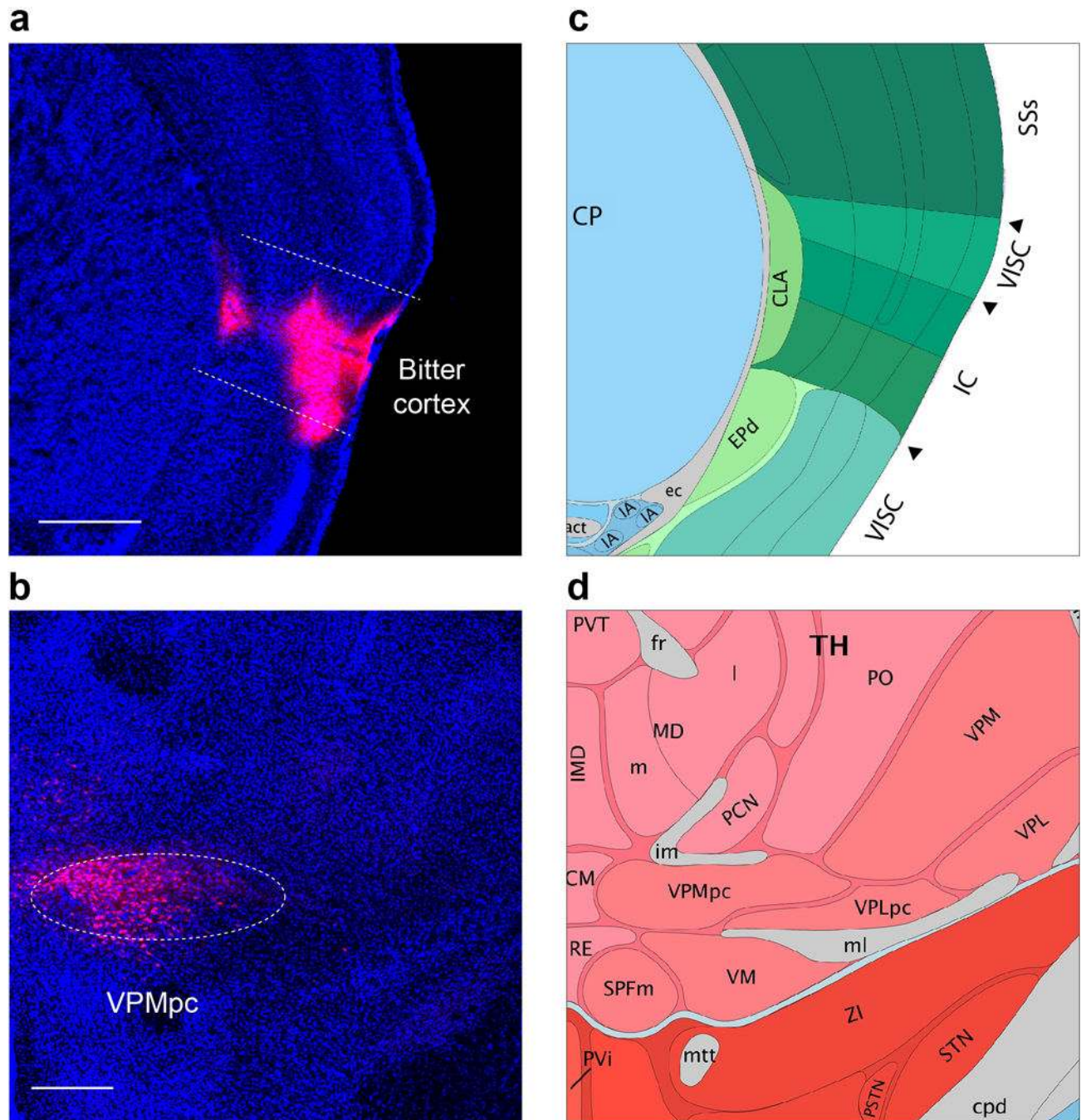
Extended Data Figure 7: Retrograde labeling of gustatory thalamic neurons.
a, b, Injection of the retrograde tracer cholera toxin subunit B-Alexa Fluor 594 in taste cortex (bitter cortical field, shown in red, panel **a**), selectively labels neurons in the taste thalamus (VPMpc, panel **b**). Similar results were observed in 2 animals. **c,d**, Diagrams of the corresponding brain regions, adapted from the Allen Brain Institute atlas. Scale bars, 500 μm.
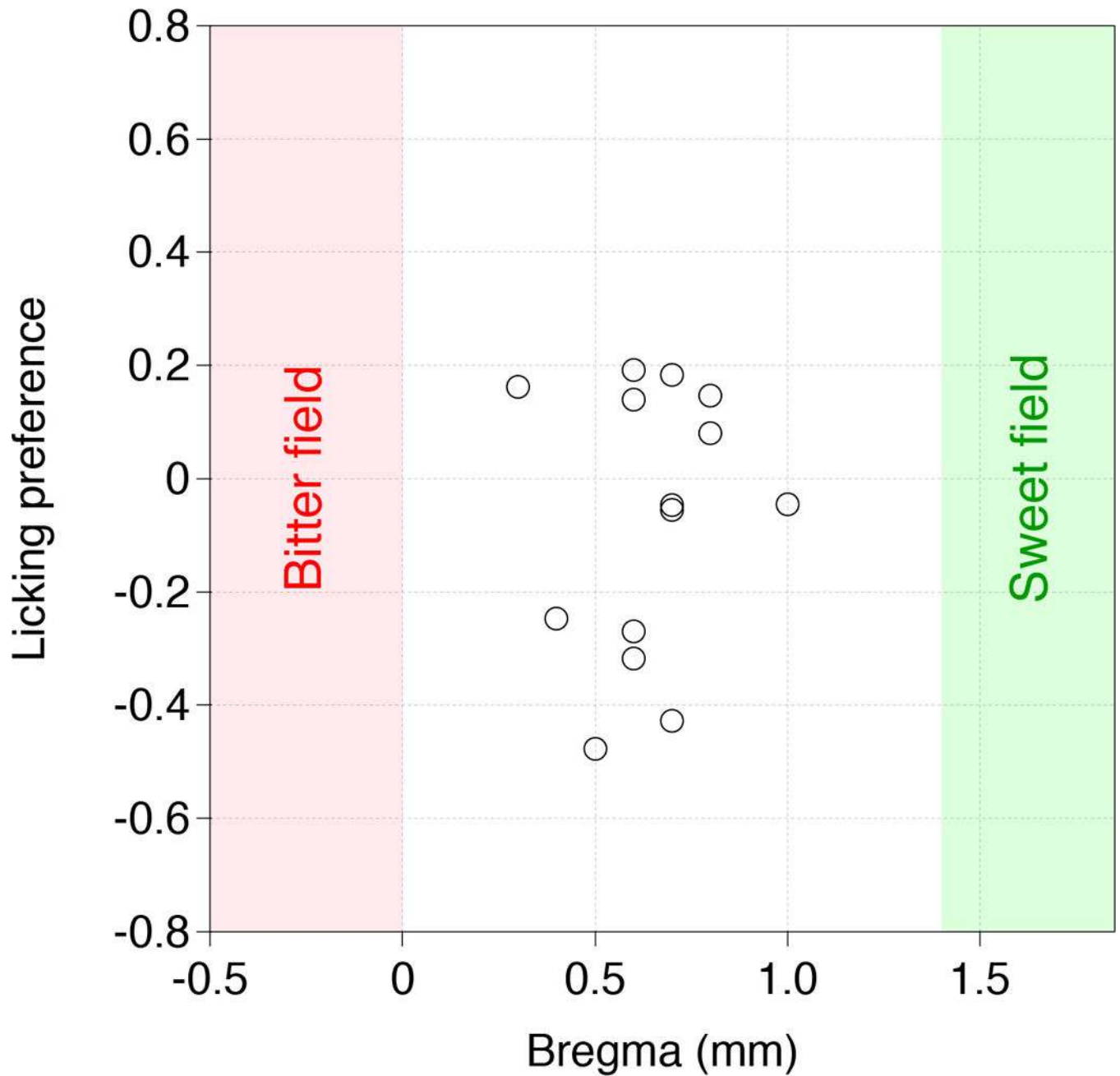
Extended Data Figure 8: Licking responses to photostimulation of intermediate regions between sweet and bitter cortex.

Shown are behavioral responses (see Fig. 3) in water-only trials linked to contact-driven self-stimulation for mice expressing ChR2 between the sweet and bitter cortical fields. Note that a positive index means attraction, while a negative index means aversion to light stimulation. n= 14 mice. Data points indicate the behavioral test from individual animals at different stimulation sites relative to Bregma position.

Supplementary Material

Refer to Web version on PubMed Central for supplementary material.

Acknowledgements

References

1. Yarmolinsky DA, Zuker CS & Ryba NJ Common sense about taste: from mammals to insects. Cell 139, 234–244, doi:10.1016/j.cell.2009.10.001 (2009). [PubMed: 19837029]

2. Scott K Taste recognition: food for thought. Neuron 48, 455–464, doi:10.1016/j.neuron.2005.10.015 (2005). [PubMed: 16269362]

3. Spector AC & Travers SP The representation of taste quality in the mammalian nervous system. Behavioral and cognitive neuroscience reviews 4, 143–191, doi:10.1177/1534582305280031 (2005). [PubMed: 16510892]

4. Accolla R, Bathellier B, Petersen CC & Carleton A Differential spatial representation of taste modalities in the rat gustatory cortex. The Journal of neuroscience : the official journal of the Society for Neuroscience 27, 1396–1404, doi:10.1523/JNEUROSCI.5188-06.2007 (2007). [PubMed: 17287514]

5. Yoshimura H, Sugai T, Fukuda M, Segami N & Onoda N Cortical spatial aspects of optical intrinsic signals in response to sucrose and NaCl stimuli. Neuroreport 15, 17–20, doi:10.1097/01.wnr. 0000107520.38715.21 (2004). [PubMed: 15106824]

6. Chen X, Gabitto M, Peng Y, Ryba NJ & Zuker CS A gustotopic map of taste qualities in the mammalian brain. Science 333, 1262–1266, doi:10.1126/science.1204076 (2011). [PubMed: 21885776]

7. Peng Y et al. Sweet and bitter taste in the brain of awake behaving animals. Nature 527, 512–515, doi:10.1038/nature15763 (2015). [PubMed: 26580015]

8. Susaki EA et al. Whole-brain imaging with single-cell resolution using chemical cocktails and computational analysis. Cell 157, 726–739, doi:10.1016/j.cell.2014.03.042 (2014). [PubMed: 24746791]

9. Zingg B et al. AAV-Mediated Anterograde Transsynaptic Tagging: Mapping Corticocollicular Input-Defined Neural Pathways for Defense Behaviors. Neuron 93, 33–47, doi:10.1016/j.neuron. 2016.11.045 (2017). [PubMed: 27989459]

10. Cai H, Haubensak W, Anthony TE & Anderson DJ Central amygdala PKC-delta(+) neurons mediate the influence of multiple anorexigenic signals. Nat Neurosci 17, 1240–1248, doi: 10.1038/nn.3767 (2014). [PubMed: 25064852]

11. Janak PH & Tye KM From circuits to behaviour in the amygdala. Nature 517, 284–292, doi: 10.1038/nature14188 (2015). [PubMed: 25592533]

12. Paton JJ, Belova MA, Morrison SE & Salzman CD The primate amygdala represents the positive and negative value of visual stimuli during learning. Nature 439, 865–870, doi:10.1038/ nature04490 (2006). [PubMed: 16482160]

13. Douglass AM et al. Central amygdala circuits modulate food consumption through a positive-valence mechanism. Nat Neurosci 20, 1384–1394, doi:10.1038/nn.4623 (2017). [PubMed: 28825719]

14. Kim J, Pignatelli M, Xu S, Itohara S & Tonegawa S Antagonistic negative and positive neurons of the basolateral amygdala. Nat Neurosci 19, 1636–1646, doi:10.1038/nn.4414 (2016). [PubMed: 27749826]

15. Namburi P et al. A circuit mechanism for differentiating positive and negative associations. Nature 520, 675–678, doi:10.1038/nature14366 (2015). [PubMed: 25925480]

16. Gore F et al. Neural Representations of Unconditioned Stimuli in Basolateral Amygdala Mediate Innate and Learned Responses. Cell 162, 134–145, doi:10.1016/j.cell.2015.06.027 (2015). [PubMed: 26140594]

17. Han W et al. Integrated Control of Predatory Hunting by the Central Nucleus of the Amygdala. Cell 168, 311–324 e318, doi:10.1016/j.cell.2016.12.027 (2017). [PubMed: 28086095]

18. Kim J, Zhang X, Muralidhar S, LeBlanc SA & Tonegawa S Basolateral to Central Amygdala Neural Circuits for Appetitive Behaviors. Neuron 93, 1464–1479 e1465, doi:10.1016/j.neuron. 2017.02.034 (2017). [PubMed: 28334609]

19. Beyeler A. C., Chia-Jung; Silvestre Margaux; Lévêque Clémentine; Namburi Praneeth; Wildes Craig P.; Tye Kay M.;. Organization of Valence-Encoding and Projection-Defined Neurons in the Basolateral Amygdala. Cell Reports 22, 905–918, doi:10.1016/j.celrep.2017.12.097 (2018). [PubMed: 29386133]

20. Boyden ES, Zhang F, Bamberg E, Nagel G & Deisseroth K Millisecond-timescale, genetically targeted optical control of neural activity. Nat Neurosci 8, 1263–1268, doi:10.1038/nn1525 (2005). [PubMed: 16116447]

21. Tye KM et al. Amygdala circuitry mediating reversible and bidirectional control of anxiety. Nature 471, 358–362, doi:10.1038/nature09820 (2011). [PubMed: 21389985]

22. Stachniak TJ, Ghosh A & Sternson SM Chemogenetic synaptic silencing of neural circuits localizes a hypothalamus-->midbrain pathway for feeding behavior. Neuron 82, 797–808, doi: 10.1016/j.neuron.2014.04.008 (2014). [PubMed: 24768300]

23. Maren S Neurobiology of Pavlovian fear conditioning. Annu Rev Neurosci 24, 897–931, doi: 10.1146/annurev.neuro.24.1.897 (2001). [PubMed: 11520922]

24. Cardinal RN, Parkinson JA, Hall J & Everitt BJ Emotion and motivation: the role of the amygdala, ventral striatum, and prefrontal cortex. Neurosci Biobehav R 26, 321–352, doi:10.1016/ S0149-7634(02)00007-6 (2002).

25. Schoenbaum G, Chiba AA & Gallagher M Neural encoding in orbitofrontal cortex and basolateral amygdala during olfactory discrimination learning. The Journal of neuroscience : the official journal of the Society for Neuroscience 19, 1876–1884 (1999). [PubMed: 10024371]

26. Lein ES et al. Genome-wide atlas of gene expression in the adult mouse brain. Nature 445, 168–176, doi:10.1038/nature05453 (2007). [PubMed: 17151600]

27. Bakker R, Tiesinga P & Kotter R The Scalable Brain Atlas: Instant Web-Based Access to Public Brain Atlases and Related Content. Neuroinformatics 13, 353–366, doi:10.1007/s12021-014-9258-x (2015). [PubMed: 25682754]

28. Armbruster BN, Li X, Pausch MH, Herlitze S & Roth BL Evolving the lock to fit the key to create a family of G protein-coupled receptors potently activated by an inert ligand. P Natl Acad Sci USA 104, 5163–5168, doi:10.1073/pnas.0700293104 (2007).

29. Grill HJ & Norgren R The taste reactivity test. II. Mimetic responses to gustatory stimuli in chronic thalamic and chronic decerebrate rats. Brain research 143, 281–297 (1978). [PubMed: 630410]

30. Madisen L et al. A robust and high-throughput Cre reporting and characterization system for the whole mouse brain. Nat Neurosci 13, 133–140, doi:10.1038/nn.2467 (2010). [PubMed: 20023653]

31. Susaki EA et al. Advanced CUBIC protocols for whole-brain and whole-body clearing and imaging. Nat Protoc 10, 1709–1727, doi:10.1038/nprot.2015.085 (2015). [PubMed: 26448360]

32. Avants BB et al. A reproducible evaluation of ANTs similarity metric performance in brain image registration. Neuroimage 54, 2033–2044, doi:10.1016/j.neuroimage.2010.09.025 (2011). [PubMed: 20851191]

33. Zhang Y et al. Coding of sweet, bitter, and umami tastes: different receptor cells sharing similar signaling pathways. Cell 112, 293–301 (2003). [PubMed: 12581520]

34. Kim CK et al. Molecular and Circuit-Dynamical Identification of Top-Down Neural Mechanisms for Restraint of Reward Seeking. Cell 170, 1013–1027 e1014, doi:10.1016/j.cell.2017.07.020 (2017). [PubMed: 28823561]

35. Ilango A et al. Similar roles of substantia nigra and ventral tegmental dopamine neurons in reward and aversion. The Journal of neuroscience : the official journal of the Society for Neuroscience 34, 817–822, doi:10.1523/JNEUROSCI.1703-13.2014 (2014). [PubMed: 24431440]

36. Krettek JE & Price JL A description of the amygdaloid complex in the rat and cat with observations on intra-amygdaloid axonal connections. J Comp Neurol 178, 255–280, doi:10.1002/cne.901780205 (1978). [PubMed: 627626]
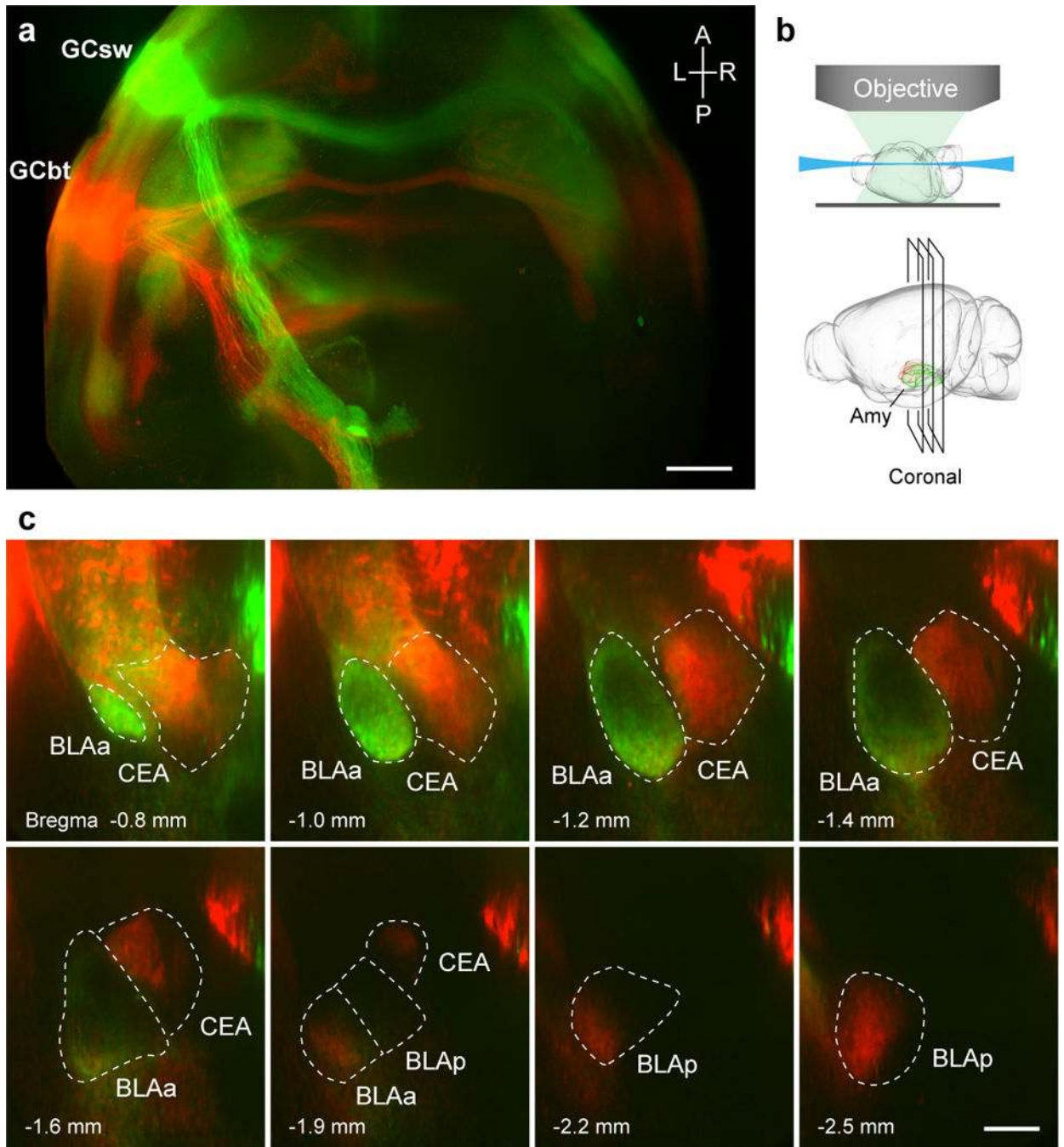
Figure 1: Projections from sweet and bitter cortex terminate in distinct targets in the amygdala.
a, Maximum-intensity Z-stack of projections[8] from the sweet cortical field labeled with eGFP (GCsw, green) and the bitter cortical field labeled with tdTomato (GCbt, red); A, anterior; P, posterior; L, left; R, right. Scale bar, 1 mm. **b**, Schematic of whole-brain imaging with light-sheet fluorescence microscopy[8], illustrating the coronal sections shown in c. Amy, amygdala. The brain diagrams were rendered by the Scalable Brain Composer (https://scalablebrainatlas.incf.org/services/sba-composer.php?template=ABA_v3) based on Allen Mouse Brain Common Coordinate Framework version 3[26,27]. **c**, Segregation of sweet and

bitter projections. Sweet cortical neurons project to anterior basolateral amygdala (BLAa, green), while bitter cortical neurons predominantly innervate central amygdala (CEA, red), and to a portion of posterior basolateral amygdala (BLAp, red; see also Extended Data Fig. 1). Scale bar, 0.5 mm. The boundaries of amygdala nuclei were based on the Allen Brain Institute atlas[26] (http://brain-map.org/). Similar results were observed in 6 animals.
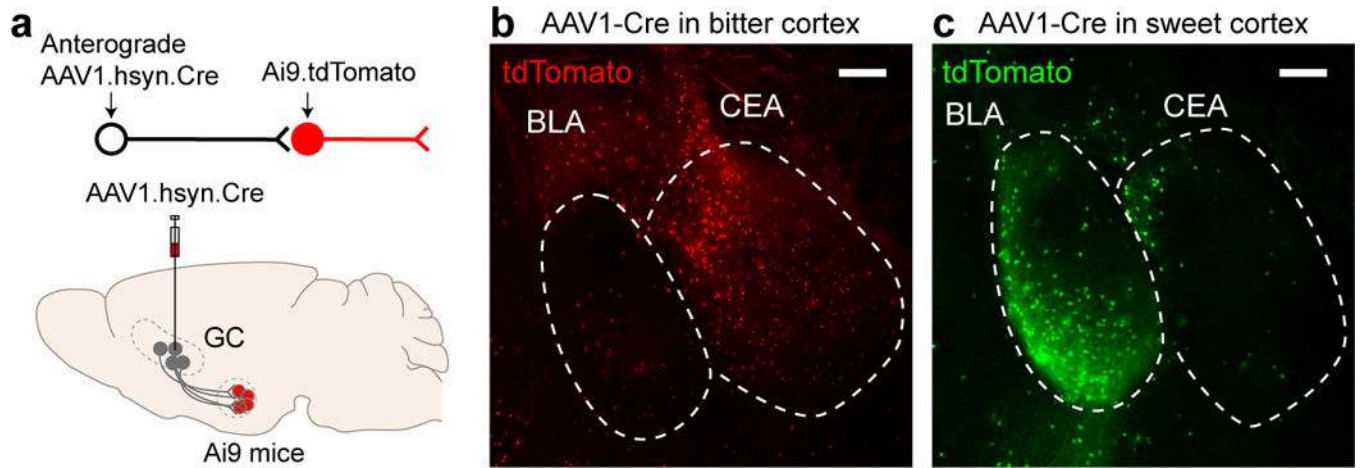
Figure 2: Segregation of sweet and bitter targets in the amygdala.
a, Schematic illustrating anterograde transsynaptic labeling of amygdalar neurons following AAV1.hsyn.Cre injection[9] in the sweet or bitter taste cortex of animals carrying a tdTomato reporter. **b-c**, Representative confocal images of tdTomato expression in amygdala following AAV1 injection in (**b**) bitter cortex or (**c**) sweet cortex (pseudocolored green). Scale bars, 200 μm. Similar results were obtained in 3 animals for each experiment. See also Extended Data Fig. 2.
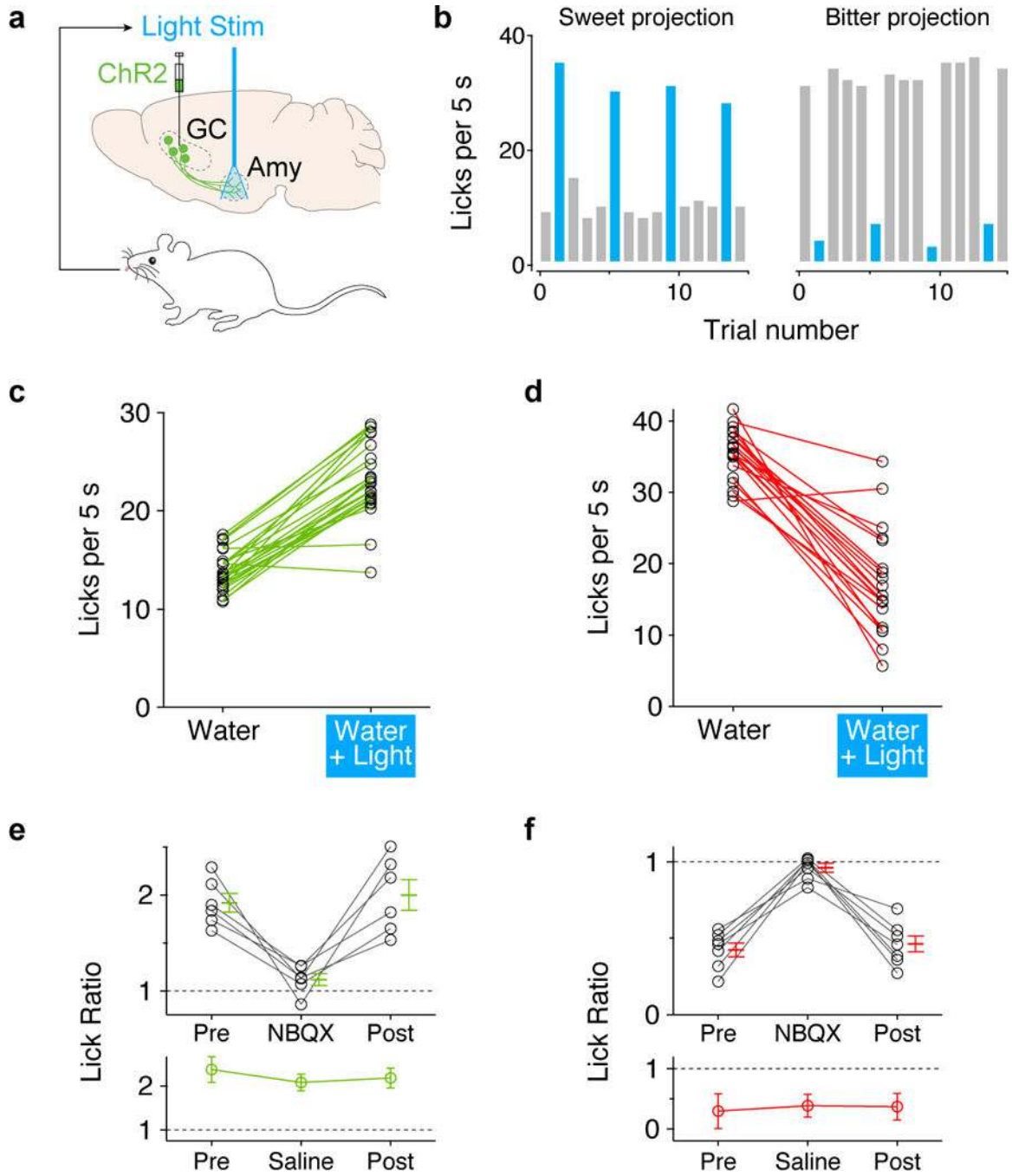
Figure 3: Activation of sweet and bitter cortical terminals in amygdala drives appetitive and aversive behaviors.

a, Optogenetic stimulation strategy. Sweet neurons in anterior gustatory cortex (GC) or bitter neurons in posterior GC were transduced with AAV-ChR2. Stimulating optical fibers were placed above BLA or CEA. Amy, amygdala. For coupling the photostimulation to drinking behavior, laser pulses were triggered by the animal's licking. **b**, Representative histograms showing licking events in the presence (blue) or absence (grey) of photostimulation of sweet cortico-amygdalar projections (left panel) or bitter cortico-amygdalar projections (right

panel). Note the dramatic enhancement, or suppression of licking, respectively. **c-d**, Quantitation of licking responses with and without light stimulation; **c**, sweet cortical terminals in BLA (n=24 mice, two-tailed paired t-test, P<0.0001); **d**, bitter cortical terminals in CEA (n=21 mice, two-tailed paired t-test, P<0.0001). See also Extended Data Fig. 4. **e-f**, Pharmacological silencing demonstrated that the light-dependent licking behaviors are due to activity in the amygdala; the panels show quantitation of lick ratios before and after infusion of NBQX (upper) or control saline (lower) in amygdala. Panel e, stimulation of sweet projections (n=6 mice); panel f, stimulation of bitter projections (n=7 mice). Note that NBQX abolishes the light-dependent changes in licking responses. Values are mean ± s.e.m. Repeated measures one-way analysis of variance (RM one-way ANOVA) followed by Bonferroni post-hoc test was used in the analysis (Supplementary Table 1).
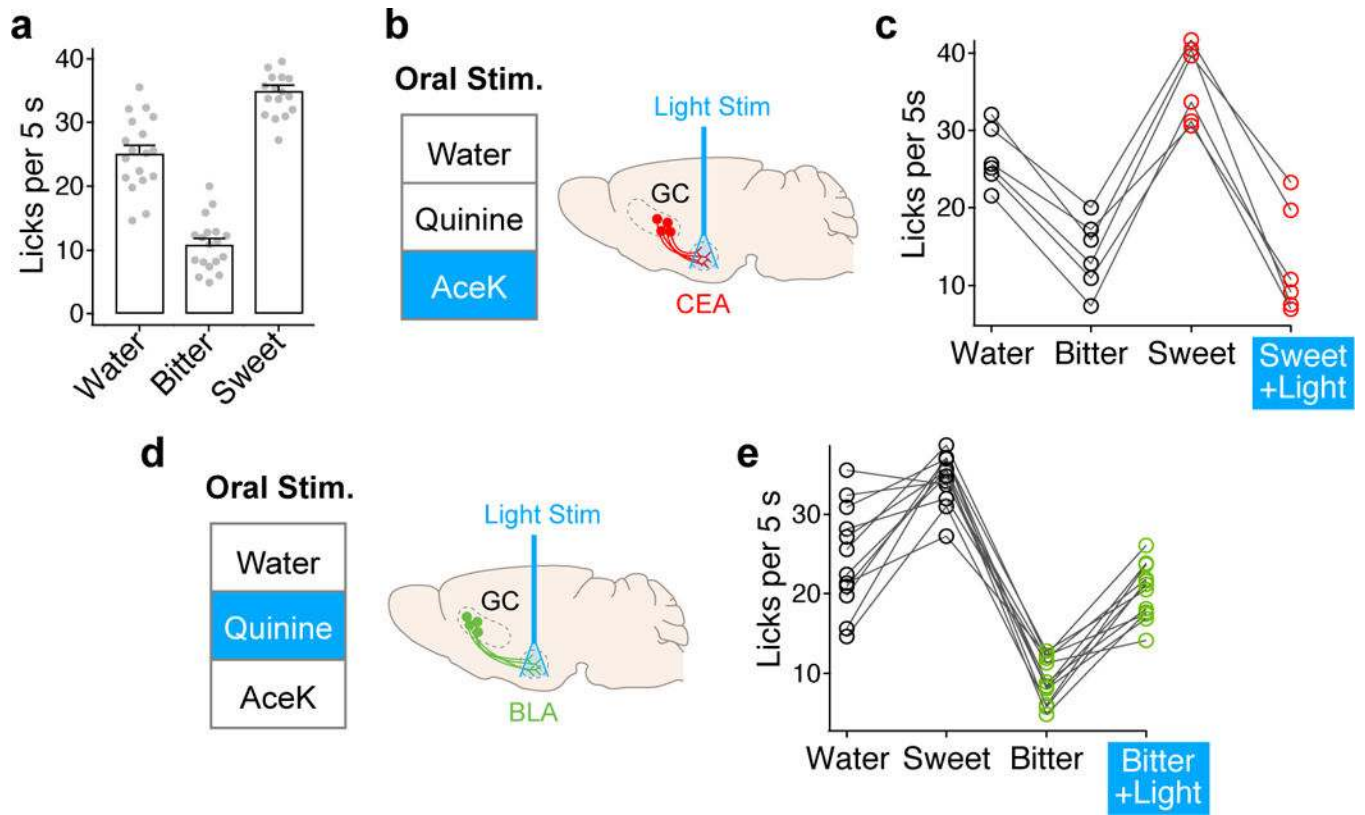
Figure 4: Activation of cortico-amygdala circuits overrides the hedonic valence of orally delivered tastants.

a, Licking responses (no photostimulation) to water, bitter (0.5 mM quinine) and sweet stimuli (4mM AceK); n=18 mice; mean ± s.e.m. **b**, Schematic of optogenetic stimulation strategy; AAV-ChR2 was injected into the bitter cortex and the optical fiber was placed above CEA. **c**, Quantitation of licking response to water, bitter, sweet, and sweet + light; n=6 mice; stimulation overrides the attractive responses to the sweet stimulus. **d**, Schematic of photostimulation of sweet terminals. **e**, Quantitation of licking response to water, sweet, bitter, and bitter + light; n=12 mice; stimulation overrides the aversive responses to the bitter stimulus. RM one-way ANOVA followed by Bonferroni post-hoc test; see Supplementary Table 1.
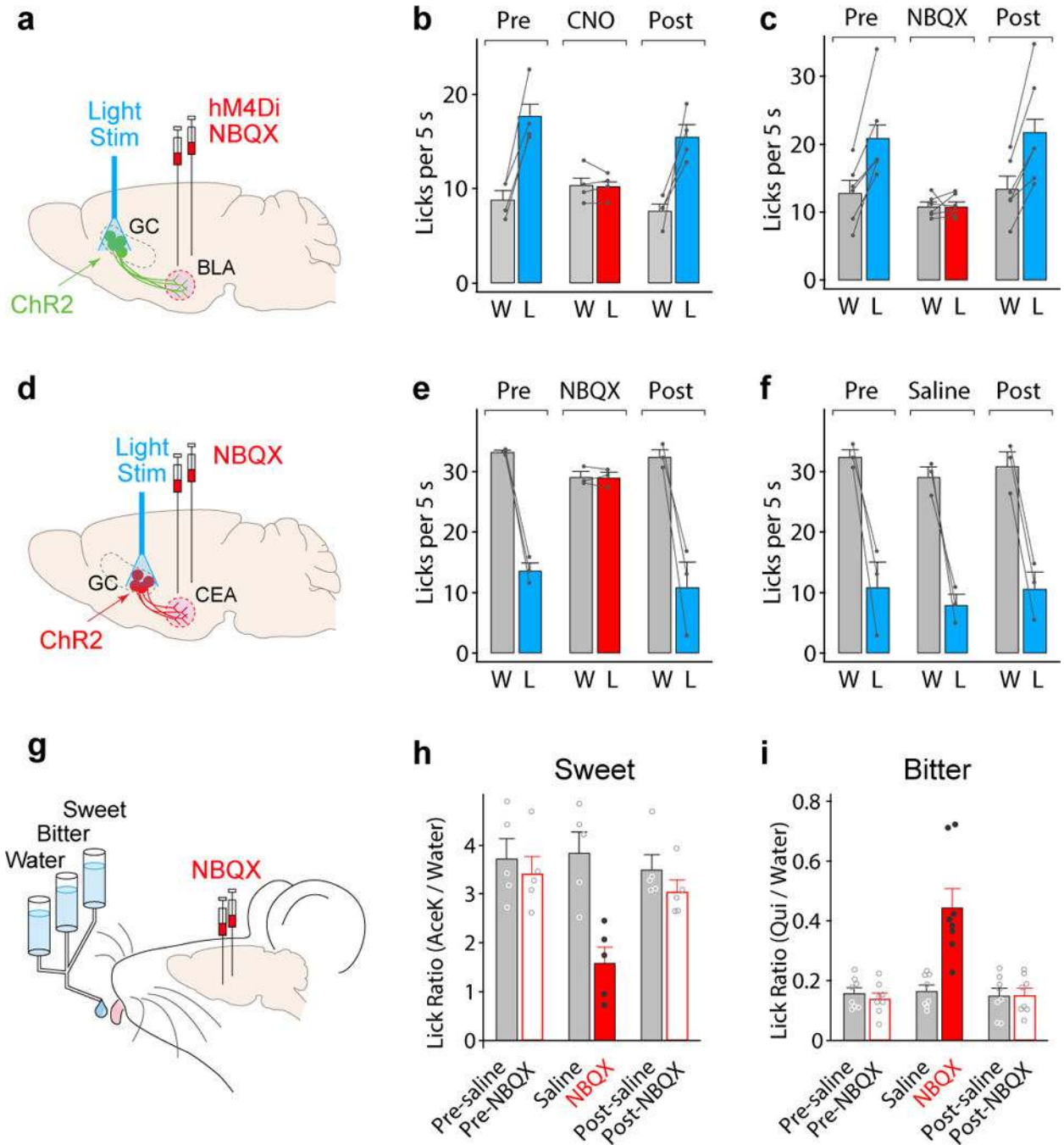
Figure 5: Silencing the amygdala impairs taste valence.
a, Schematic of optogenetic stimulation and chemogenetic/pharmacological silencing strategy. AAV-ChR2 was injected unilaterally into sweet cortex, and an optical fiber implanted for photostimulation. AAV-hM4Di[28] was targeted bilaterally to BLA for chemogenetic silencing (alternatively, cannulas were implanted bilaterally over the amygdala for pharmacological silencing). **b**, Chemogenetic silencing the amygdala with inhibitory DREADD (hM4Di) and clozapine N-oxide (CNO) abolished the strong appetitive behavior observed following photostimulation of sweet cortex (compare Pre and Post with

CNO); n=4 mice, water (W) vs. water + light (L), two-tailed paired t-test, Pre: P=0.0054, CNO: P=0.8900, Post: P=0.0265. See Extended Data Fig. 5 for controls. **c**, Pharmacological silencing the amygdala with NBQX similarly abolished the appetitive behavior associated with photostimulation of sweet cortex; n= 6 mice, two-tailed paired t-test, Pre: P=0.0049, NBQX: P=0.9458, Post: P=0.0042. See Extended Data Fig.5 for controls. **d,e**, NBQX silencing of amygdala abolished aversive responses to photostimulation of bitter cortex; n=3 mice, two-tailed paired t-test, Pre: P=0.0047, NBQX: P=0.9125, Post: P=0.0261. **f**, Saline controls for NBQX silencing following photostimulation of bitter cortex. n=3 mice, two-tailed paired t-test, Pre: P=0.0261, Saline: P=0.0230, Post: P=0.0005. **g,h,i**, NBQX silencing of amygdala severely diminished attraction to sweet (n=5 mice) and aversion to bitter chemicals (n=8 mice); the small remaining responses to the orally applied sweet and bitter tastants likely reflect brain-stem dependent immediate reactions to taste observed in decerebrated animals[29]. RM one-way ANOVA followed by Bonferroni post-hoc test (Supplementary Table 1). Values are mean ± s.e.m.
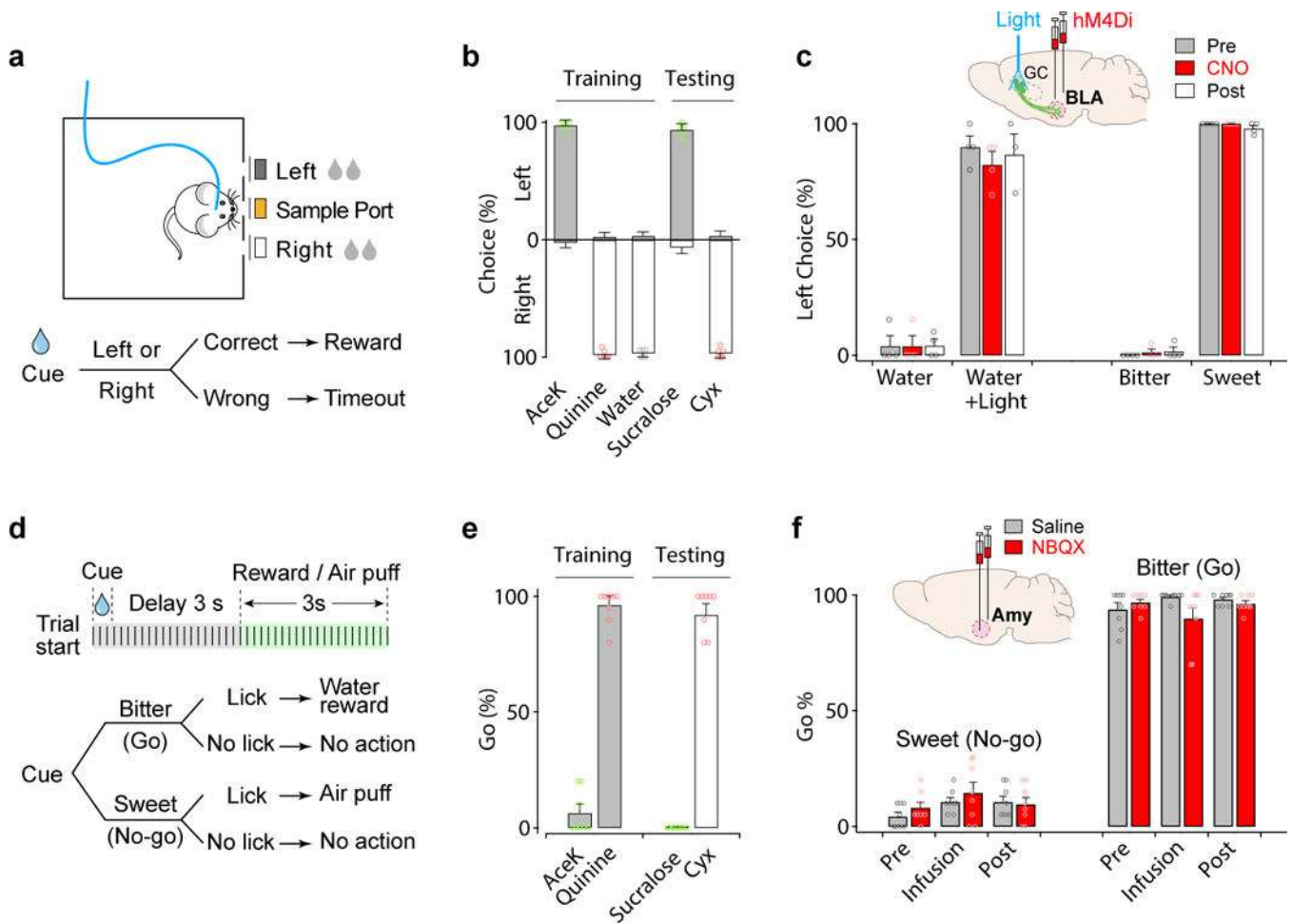
Figure 6: Silencing the amygdala does not prevent tastant recognition.

a, Schematic and flow chart for the three-port taste recognition task. In each trial, a mouse had 0.5 s to lick a randomly presented taste cue from the middle port, and then go to either left or right to report the identity of the tastant (in this example mice were trained to go left for sweet and right for bitter or water); correct responses were rewarded with 4s of water, while incorrect ones led to a 5s timeout penalty. **b**, Quantitation of results from three-port recognition sessions, demonstrating highly reliable recognition of the stimulus identity (>90% accuracy; n=6 mice); concentrations: 10 mM AceK, 1 mM quinine, 3 mM sucralose, 10 μM cycloheximide (Cyx). **c**, The animals used in Fig. 5b were assayed for the effect of silencing amygdala (n=4 Pre, CNO; n=3 Post). Animals with silenced amygdala can still identify the different tastes with normal accuracy. Importantly, photostimulation of sweet cortex is recognized as a sweet tasting stimuli[7], and remains so after CNO silencing of amygdala (compare water vs. water + light). The graph only presents the responses to the left port (i.e. sweet identity). **d**, The animals used in Fig. 5e,h,i were assayed using Go/No-go tastant recognition tests[7]. Panel **e** demonstrates highly reliable recognition of the stimulus identity after training (>90% accuracy; n=8mice). Concentrations: 4 mM AceK, 1 mM quinine, 3 mM sucralose, 10 μM Cyx. **f**, Pharmacological silencing of amygdala (Amy) has no significant effect on either sweet or bitter recognition (n=8 mice). Two-way or RM one-

way ANOVA followed by Bonferroni post-hoc test (Supplementary Table 1). Values are mean ± s.e.m.